BUCKLING OF A STRIP ON A RIGID HALF-SPACE WITH A TRANSVERSE PRESSURE : WRINKLING OF NON-BONDED CLADDING

W.F. ANDERSON,

Liquid Metal Engineering Center, Canoga Park, California, U.S.A.

ABSTRACT

The problem investigated is that of the stability of a uniform strip resting on a rigid half-space as a base while subjected to both a transverse force pressing it against the base, and an axial force or displacement.

The system is shown to be completely imperfection-sensitive, with theoretically infinite buckling loads in the absence of imperfections. The behavior of the strip after buckling ensues is highly nonlinear. The effect of both sharp and smooth (cosine wave) imperfections is studied analytically. A numerical method is also developed for solution of the static buckling problem. Results of the analytical and numerical methods agree.

The numerical method is used to obtain the static buckling load where the base has uniformly distributed imperfections of random magnitude. Forty-nine cases of buckling, with the base having random imperfections, are studied and a correlation is shown between the magnitude of the axial buckling force and the RMS value of the magnitude of the random imperfections.

1. INTRODUCTION

Most structural systems which include a beam or plate members supported by a surface are idealized for analysis as being supported by an elastic foundation capable of tension at the surface. In this study the foundation is considered to be rigid, and a study is made of the buckling behavior of the cladding or some other member being supported by a tensionless surface. In this structural system there is a transverse force induced by pressure or gravity which tends to hold the cladding or other member against the rigid surface. In-plane forces on the cladding are generally induced by the forcing of geometric compatibility under conditions of differential thermal expansion or different initial dimensions.

In previous work, Anderson [1] studied the one-dimensional problem of buckling of an axial strip of cladding along a container with a net external pressure and relatively rigid contents.

*Technical Advisor, Liquid Metal Engineering Center, P. O. Box 1449, Canoga Park, Calif. 91304

A simplified plastic model of the buckled configuration was also studied by Anderson [1]. The existence of three plastic hinges was assumed, one at the crest and one at each point of contact with the base. The results predicted by this study agreed with observed buckles.

Calladine [2] studied the creep behavior of buckles in the cladding on a circular cylindrical rod. He assumed an initial buckled configuration and used both analytical and numerical methods to predict its subsequent time-dependent behavior.

The problem of a ring constrained in a rigid circular cavity is similar to the problem of a strip held against a rigid flat surface by transverse pressure. This later problem has been the subject of several recent investigations [3 - 9]. Experimental results were reported by Elkon [5] and by Chann and McMinn [6].

Anderson [10] studied the effect of friction on buckling of a flat strip and devised numerical methods for both static and dynamic solutions. Weitsman [11] studied several examples of a beam or plate subjected to a concentrated force and supported on the tensionless surface of an elastic foundation.

2. STATEMENT OF THE PROBLEM

The strip is considered to be of unit width and uniform thickness. The ratio of thickness to width is such that the bending stiffness is approximated by bending stiffness expressions for a flat plate. Otherwise, the Kirchhoff assumptions associated with the strength-of-materials approach to beam problems are considered to be effective, including those of small deformations and small deflections.

Specific assumptions concerning the effect of sharp changes of contact of the strip with the base are as follows:

a) Abrupt changes in contact with the base are assumed to occur.

b) Local deformations in the strip resulting from abrupt changes of contact with the base are assumed negligible.

c) The base is assumed to be rigid, admitting no deformations at abrupt changes in contact with the strip.

d) At points of change in contact between the strip and a relatively smooth base, both the transverse displacement and the slope of the strip must coincide with those of the base. Exceptions to this occur at isolated or distributed sharp imperfections in the surface of the base, or at the point of contact between contiguous buckles, at which points only the displacements must coincide.

e) If contact between the strip and the base occurs over a finite length, the displacement, slope, and curvature of the strip must coincide with the displacement, slope, and curvature of the boundary of the base throughout the length of contact and at the points of change of contact.

f) The axial force P is constant in x.

g) The pressurizing medium is uniform and has only a Z component.

The preceding assumptions allow the static equilibrium of the strip to be described by following the equations as derived by Timoshenko and Gere [12] and referring also to Figure 1 (a and b) to yield:

$$dV/dx = -q + r \tag{1}$$

and

$$V = M' - Pw' \tag{2}$$

which, with P as a constant and

$$M = -D(w'' - w''_{so}) \ , \tag{3}$$

yield the equation of equilibrium for a general element not in contact with the base as

$$D(w'''' - w''''_{so}) + Pw'' = q \ , \tag{4}$$

with x in the domain $-S < x < S$ and w in the range $w(x) \leq w_b(x)$, where

$w = w(x)$ = total deflection of the strip

$w_b = w_b(x)$ = configuration of the base

$w_{so} = w_{so}(x)$ = stress-free configuration of the strip

$M = M(x)$ = bending moment in the strip

$P = P(x)$ = axial force in the strip

$V = V(x)$ = transverse shear force in the strip

D = bending rigidity of the strip, a constant

q = the transverse pressure, a constant

h = thickness of the strip, a constant.

In general the subscript s denotes a value of a variable at $x = s$.

While eq. (4) for w(x) appears to be linear, the restraints on the range of w cause the system to be classified as non-linear.

In the mathematical solutions, instability is defined to occur where an increasing buckle height (or length) may be supported by a constant or decreasing axial force.

The equilibrium method is used to investigate stability of the system by determining if there exist any non-trivial positions of static equilibrium. For instability to occur, such non-trivial positions must exist as adjacent points, thus defining bifurcation points, to the trivial position.

When the perfect system does not show a bifurcation point or a limiting load on the perfect system at which instability occurs, the system must be studied for the effect of imperfections as was done in [4 - 7] for the ring in a rigid cavity. In the mathematical study, the imperfections are introduced into the supporting surface. Two types of imperfections are studied: (a) a point imperfection, and (b) a smooth, cosine wave imperfection. The effect of reducing the size of the imperfection to zero is studied as the limit case for a perfect system.

In the numerical solutions, instability is defined to occur when the axial velocity and acceleration of the displacement of the end of the strip are both positive toward the center under constant axial force.

3. MATHEMATICAL ANALYSIS OF A BUCKLE

3.1 General Equation for a Buckle

Considering that the strip is initially straight in a stress-free state yields $w_{so} \equiv 0$. Eq. (4) then becomes

$$Dw'''' + Pw'' = q \quad \text{for} \quad -S < x < S \quad . \tag{5}$$

Assuming the buckle is symmetrical about $x = 0$ yields the boundary conditions $w' = w''' = 0$ at $x = 0$. Integrating eq. (5) twice over the range $0 \leq x \leq S$ yields a second-order differential whose total solution has

$$w(x) = A \sin kx + B \cos kx + (PW_o - M_o)/P - qD/P^2 + qx^2/2P \quad , \tag{6}$$

with

$$k^2 = P/D \quad , \tag{7}$$

and $W_o = w(x)$ at $x = 0$. A and B are unknown constants, with $A = 0$ by the symmetry.

The boundary conditions at the end of the buckle, $x = S$, are $w = w_s$, $w' = w'_s$, $-Dw'' = M_s$. Moment equilibrium yields $M_s - Pw_s = M_o - PW_o - qS^2/2$.

Substituting the above into eq. (6) yields two equations in B. Dividing one of these by the other to eliminate B yields the general characteristic equation

$$\frac{k \sin kS}{\cos kS} = \frac{qS - Pw'_s}{(q/k^2) + M_s} \quad . \tag{8}$$

3.2 Equilibrium Buckles in a Perfect System

In the perfect system, the strip lies on base stress-free with no imperfections in either strip or base; $w_{so} \equiv 0$ and $w_b \equiv 0$. A buckle extending over the range $-S < x < S$ will then have, as shown in Figure 1a, $w < 0$ for $-S < x < S$. The boundary conditions at the ends of the buckle are $w' = w = 0$ at $x = \pm S$.

One may postulate the existence of multiple contiguous buckles, or a buckle over the full length of the strip. Therefore, the curvature w''_s and moment M_s will not be held to zero value.

Using these boundary conditions, the values of kS which satisfy the characteristic equation are in the range $\pi < kS \leq 4.4934$ for $\infty > M_s \geq 0$. For all short isolated buckles with $S < L/2$ and $M_s = 0$, the value of kS is a constant, $kS = 4.4934$ in the lowest buckling mode. The next higher mode has $kS = 7.7253$. No constant value can be determined for either k or S independent of the other; the length of the buckle remains a variable.

After substituting into eq. (6) for A and B, w(x) is expressed by

$$w = \frac{-q}{Pk^2}\left(1 + \frac{k^2 M_s}{q}\right)\left(1 - \frac{\cos kx}{\cos kS}\right) - \frac{q}{2P}\left(S^2 - x^2\right) \quad . \tag{9}$$

By substituting from eq.(7) into eq.(9) with x = 0, one obtains for P as a function of W_o

$$\frac{P}{(2\pi/L)^2 D} = \left(\frac{q}{W_o D}\right)^{1/2} \cdot \frac{1}{(2\pi/L)^2} \left\{ \left[1 - \frac{(kS)^2}{\pi^2} \cdot \frac{(DW_o)}{q} \cdot \frac{(2\pi)^4}{L^4} \cdot \frac{w''_s}{\frac{(2\pi)^2}{L^2} W_o} \right] \cdot \left[1 - \frac{1}{\cos kS} \right] - \frac{(kS)^2}{2} \right\}^{1/2} . \qquad (10)$$

For short, isolated buckles with $M_s = 0$ and kS = 4.4934, eq.(10), becomes

$$-W_o = \frac{-15.7\, qS^4}{D(kS)^4} = \frac{-15.7\, qD}{p^2} = \frac{-0.0385\, qS^4}{D} , \qquad (11)$$

and under these conditions either the length S or the center deflection W_o is a suitable measure for the magnitude of a given mode shape.

The relations of the axial force P to W_o and to the length of the buckle S, as expressed by eqs.(10) and (11) are shown graphically in Figure 2 for the full range of S including S = L/2 and $M_s > 0$. It can be seen that the value of P approaches infinity as the size of the buckle approaches zero.

3.3 Solution for a Buckle at a Point Imperfection

A short isolated symmetrical buckle is assumed, with the strip being stress-free while straight. There is assumed to be a point imperfection at x = 0 so that $w_b = -W_i \delta(x)$. The boundary conditions at the end of the buckle are then $w = w' = w'' = 0$ at x = S; and at the center while the strip is in contact with the imperfection $w' = 0$ and $V_o = -Dw'''_o = F_i/2 \geq 0$ at x = 0, where F_i is the force in the -Z direction exerted by the point against the strip. V_o and F_i vary with S, P, and W_i but neither F_i nor W_i are allowed to assume negative values.

Eq.(5) is integrated twice over the range $0 \leq x \leq S$ and solved to yield two simultaneous equations with F_i and W_i as unknowns. The solution of these yields

$$F_i = \frac{2q}{k}\left(\frac{\sin kS - kS\cos kS}{1 - \cos kS}\right) \qquad (12)$$

and

$$W_i = \frac{-qD}{p^2}\left[2 + \frac{(kS)^2}{2} + kS\left(\frac{kS\cos kS - 2\sin kS}{1 - \cos kS}\right)\right] \qquad (13)$$

with $k^2 = P/D$ from eq.(7).

The value of $F_i/(k/2q)$ and $-W_i P^2/q^2 D$ can be plotted as a function of kS to show the relation between W_i and kS and also between F_i and kS for constant values of k, p, q, and D. From such a plot it can be observed that $F_i = 0$ when the values of kS and displacement W_i are the same as those of the equilibrium-free buckle of a perfect system with identical P, D, and q. It can also be seen from eq.(13) that for $F_i = 0$, when kS = 4.493, the value of P must approach infinity when W_i approaches zero.

3.4 Solution for a Buckle at a Cosine Wave Imperfection

In this case the base is presumed to have its free surface in the form of cosine waves such that the surface can be expressed by

$$w_b(x) = -W_{bo} \cos \frac{2\pi x}{L} \tag{14}$$

Buckles can be considered to form at the crests as shown in Figure 3, with equilibrium forces as noted in Figure 1b. The strip is assumed to be initially straight and then deflected to conform to the base by the pressure.

The initial phase of the strip lifting from the base can be evaluated from the equilibrium equation by substituting from eq. (14) into eq. (5). Solving for the axial force P, which will cause the contact force to become zero at the crest, yields

$$P = \frac{q}{(2\pi/L)^2 W_{bo}} + D(2\pi/L)^2 \tag{15}$$

The value of L which yields the minimum value of P is

$$L\,(\min) = 2\pi \left(\frac{D W_{bo}}{q}\right)^{1/4} = \lambda \tag{16}.$$

Arbitrary wave lengths L are related to λ by a constant C such that

$$\frac{2\pi}{\lambda} = C\left(\frac{2\pi}{L}\right) = \left(\frac{q}{D W_{bo}}\right)^{1/4} . \tag{17}$$

The value of axial force for initial lifting is

$$P = \left(\frac{2\pi}{L}\right)^2 \cdot D \cdot (1 + C^4) \quad , \tag{18}$$

and P is a minimum with C = 1 and L = λ at P = $2D(2\pi/L)^2$.

It can be seen from eq. (15) that, as with the point imperfections, the force P tends toward infinity as W_{bo} tends toward zero.

For evaluation of the relation of the transverse deflection to the axial load for the system with cosine imperfections, solutions to eq. (5) must be obtained. Again a symmetrical buckle is assumed with the conditions $w' = w''' = 0$ at $x = 0$, and at $x = \pm S$, w_s, w_s', and w_s'' are equal to the displacement, slope, and curvature of the base at that point.

Substituting for w_s', M_s, and λ into the characteristic equation with some manipulation yields the characteristic equation

$$\tan kS = kS \left[\frac{C^4 (2\pi S/L)^2}{(kS)^2} - \frac{\sin (2\pi S/L)}{(2\pi S/L)}\right] \Bigg/ \left[\frac{C^4 (2\pi S/L)^2}{(kS)^2} - \cos (2\pi S/L)\right] \tag{19}$$

The characteristic value kS in this case is not a constant, as it is with a point imperfection, but is a function of C and the relative length of the buckle as $2\pi S/L$.

Figure 4 shows the relation of kS which satisfies eq. (19) for the relative length $2\pi S/L$ for values of C = 0.5, 1.0, and 2.0.

In the region of small S, k is given approximately by $P = k^2 D = (2\pi/L)^2 D(1 + C^4)$, which agrees with eq. (18).

It can also be seen in Figure 4 that for the cosine waves with a lower magnitude of W_{bo} (larger values of C), the value of kS increases asymptotically to the value 4.4934 as S approaches L/2. This tends toward agreement with the value of kS for a buckle on a flat surface.

The values of kS were obtained by iterative solutions of eq. (19) using a digital computer program. The expression for w(x) for $0 \leq S < L/2$ is obtained from eq. (6) by substituting, and then is non-dimensionalized to

$$\frac{w_x - w_s}{W_{bo}} = -\left\{\left[C^4\left(\frac{2\pi S}{kS \cdot L}\right)^4 - \left(\frac{2\pi S}{kS \cdot L}\right)^2 \cdot \cos\frac{2\pi S}{L}\right]\left(1 - \frac{\cos kS}{\cos kS}\right) + \frac{C^4}{2} \cdot \frac{(2\pi S/L)^4}{(kS)^2}\left(1 - \frac{x^2}{S^2}\right)\right\} \cdot \qquad (20)$$

Numerical difficulties in the computations for the value of kS, even using double precision, prohibit drawing definite conclusions about the behavior of the strip at very low values of C and at very low values of S/L for high values of C.

The axial force-deflection relations for values of C = 0.5, 1.0, 2.0, and 3.0 and for a strip on a flat surface are shown in Figure 5. The force required for initial lifting and the critical buckling force as a function of C and W_{bo} are shown in Figure 6.

To allow comparison of the effect of point imperfections and cosine wave imperfections, the axial force-imperfection height relations for a point imperfection can also be expressed in terms of C and W_i with $W_i = 2W_{bo}$ from eqs. (11) and (18) as

$$\frac{P}{(2\pi/L)^2 D} = \sqrt{\frac{15.7}{2}}\left(\frac{q}{W_{bo} D}\right)^{1/2} \cdot \frac{1}{(2\pi/L)^2} = \sqrt{\frac{15.7}{2}} \cdot C^{-2} \quad . \qquad (21)$$

This relation is also shown in Figure 6.

4. NUMERICAL SOLUTIONS FOR BUCKLES

4.1 Method Used

The numerical method which was attempted and found to be successful in obtaining solutions is a simple modification of the Gauss-Seidel iterative procedure of solving sets of finite difference equations as given by Varga [13]. The calculation of the estimated value of w_i at the $(j + 1)^{th}$ iteration is done in the usual way using the $(j + 1)^{th}$ estimate of $w_k (k = 1, i - 1)$ and the $(j)^{th}$ estimate of $w_m (m = i + 1, N)$.

After calculating the $(j + 1)^{th}$ estimate of the value w_i, the modification to the Gauss-Seidel method is introduced. The estimate of w_i is tested against a restraint, the base configuration w_{bi}, and it is required that $w_i \leq w_{bi}$. If the restraint is exceeded, the estimate of w_i is set equal to the value of the restraint. In this way, all of the values of w_k and w_m which are used in forming the new estimate of w_i also satisfy the restraint condition.

The iterative method of solution of the equations of elasticity usually converges slowly and factors are applied to the new estimates to accelerate convergence as studied by White [14]. Therefore, convergence can be assured for this method by deliberately slowing the convergence process with low values of the convergence factor.

The stability calculation is based on the assumption that each cycle of the iterative process can be related to a finite time step in a numerical dynamic solution based on the predictor method. Within this assumption, finite difference derivatives with respect to the number of cycles in the iterative process can be related to finite difference derivatives in time. The validity of this assumption is demonstrated and evaluated in the Appendix. In addition, the numerical method is subject to numerical instability, which is also discussed in the Appendix. Rates of end displacement for the determination of buckling are based on intervals of ten iterative cycles to provide large differences and help to reduce the round-off error which occurs in determining the rates at each cycle.

4.2 Confirmation of the Numerical Method

The numerical method was tested by comparing the results for specific cases which were analyzed by using both numerical methods and mathematical analysis.

The case taken for an example was that of a system with the following characteristics: $E = 10.8 \times 10^6$ lb/in.^{2}; D = 1.0 lb/in.; h = 0.010 in.; q = 10 psi; L = 10 in.; W_i = 0.000134-in. height of imperfection.

A numerical solution using 299 internal nodes indicated stability of the system at P = 1050 lb and instability at P = 1100 lb, compared to P_{cr} = 1080 lb obtained mathematically.

The equilibrium configuration of a large buckle for this same system was studied using only 49 internal nodes. The stable large buckle for this system with an applied strain of ϵ_o = 0.010 in./in. is mathematically predicted to be 0.282 in. high with S = 0.925 in. as a half length. The applied strain is just sufficient to precipitate a buckle from the given imperfection. After 30 iterations with the convergence factor = 0.20, the numerical method indicated a peak deflection of 0.283 in.; and after 100 iterations, the peak deflection was 0.277 in. with a half-length of 4 nodes or approximately 0.8 in.

These results are considered as the major confirmation of the numerical method used for solving static stability problems for this system, and also as mutual confirmation of both the mathematical and numerical method.

4.3 A Strip on a Base with Random Imperfections

4.3.1 The Computer Program

The program for obtaining static solutions was developed to study the behavior of a strip on a base with random imperfections. This study concentrates on determining the buckling characteristics of a strip held against a rough surface by an applied transverse force while subjected to an axial force. The roughness of the surface is simulated by defining the configuration of the surface of the base using a set of random numbers as surface coordinates at regular intervals along the length. Variations in roughness of the base are simulated by modifying the range of the set of random numbers or by changing the length of the interval between them.

Iterations are performed by progressing through the system of equations in opposite directions on alternate cycles. This is to avoid continuously forcing the effect of imperfections toward one end of the strip.

/

4.3.2 The Cases Investigated

The system for all cases is divided into 300 segments with 299 internal nodes. A Gaussian distribution of the magnitude of random imperfections was used in all cases. Spacing between the specified imperfection points is 1, 2, 5, or 10 nodal points. In any one set, the spacing is uniform.

The magnitude of the standard deviation of the imperfections is varied by a geometric progression specified as 5 steps of magnitude per decade over greater than 2 decades for each set of spacing of imperfections.

All cases analyzed have the following system characteristics: D = 1 lb/in.; q = 10 psi; L = 10 in.

The value of the standard deviation of the imperfections ranges from 0.00001 in. to 0.00398 in., with the peak deflection in each case having a value about three times that of the standard deviation.

The program establishes an initial test loading, either read in or calculated internally on the basis of the previous step of imperfection magnitude. Iterations are initiated and allowed to continue for a number of cycles, at which time the test for buckling is started as described previously and repeated at a specified number of iterations. If buckling occurs at the initial test loading, the test loading is reduced to 80% of this initial value. If buckling does not occur within a specified maximum number of iterations, the test load is increased by a factor (1.05 for these cases) and the process repeated. The load increasing factor is repeatedly applied after the maximum allowable number of iterations at each load is reached until such time as the buckling criterion is satisfied. The computer prints the average of the last two test loadings as the buckling load.

A subroutine of the program has the printer portray graphically the buckled configuration of the strip and the configuration of the base.

The results of all the bases investigated are listed in Table 1. The results are shown graphically in Figure 7 as the relation between buckling loads and the magnitude of the standard deviation of the imperfections for the four cases of uniform spacing of the imperfections. The buckled configuration for four extremes of magnitude and spacing of the imperfections are shown in Figures 8 through 11.

4.3.3 Evaluation of the Results

As shown in eq. (16), for given values of D, q, and W_{bo}, there is a wave length λ which yields the lowest value of buckling load P. The graphical presentations of the results show a definite tendency for the length of the buckle which is formed, as listed in Table 1, to assume the length λ which would be associated with a cosine wave imperfection at the minimum buckling load. By eq. (18) it can be predicted that for initial lifting the mean axial force is

$$P_i = \left(\frac{q D}{\varphi_i W_d}\right)^{1/2} \left(C^2 + \frac{1}{C^2}\right) , \qquad (22)$$

where φ_i is a constant. If the buckles consistently form with $L = \lambda$, then C = 1.0. For C = 1.0, from Figure 6, the upper critical load is 16.4% greater than the initial lifting load so that the mean buckling load is predicted to be

$$P_{cr} = 1.164\left(\frac{qD}{\varphi_i W_d}\right)^{1/2} \cdot 2.0 \quad . \tag{23}$$

The base configuration is controlled by a set of random numbers of Gaussian distribution with a specified standard deviation; therefore, the magnitude of the imperfection, W_{bo} above, may be redefined on the basis of the standard deviation as W_d multiplied by the scale factor φ_i to be determined for each spacing.

The predicted relation from eq. (23) for P as a function of W_d with $\varphi = 1.0$ is shown in Figure 7. It can be seen that this simple relation yields a reasonable prediction for the mean of the combined results.

The result of a statistical correlation between the values of log P_{cr} and log W_d for each spacing interval, and for the combined results are given in Table 2. It can be seen that the straight line relation on a log-log basis provides an adequate correlation, with a slight improvement by the use of a second degree polynomial for correlation.

It may also be observed, both from Figure 7 and from Table 2, that there is a definite tendency for the slope of the best fit straight line for each set to increase as N_j increases.

There is also shown in Figure 7 the predicted relation obtained by considering P_{cr} as a function of W_d with $\varphi = 1.0$ and using eq. (21) for point imperfections from a flat base. The resulting equation is

$$P_{cr} = \sqrt{15.7}\left(\frac{qD}{\varphi W_d}\right)^{1/2} \quad . \tag{24}$$

It can be seen that this provides a line parallel to the line from eq. (23). Agreement between these expressions could be obtained by a value of $\varphi = 2.9$ in eq. (24).

Some refinement of these predictions can be offered on the basis of the number of random point imperfections involved. For a normal distribution this effect can be estimated on the basis of the number of points N and on the probability, (1/N), that one point in N has a value greater than θ standard deviations. This is obtained from tables of the probability integral where, for example, 1 point in 300 can be expected to be 2.72 standard deviations from the mean, whereas only 1 point in 30 can be expected to be 1.83 standard deviations from the mean. For the bases generated, the average of the ratio of the negative peak to the RMS is 2.797, 2.573, 2.363, and 2.070 for the 1, 2, 5, and 10 node intervals, respectively.

For long buckles which span many imperfections, the difference between the extreme peak and adjacent imperfection peaks may be more relevant to the buckling force than the difference between the extreme peak and the mean. This would then tend to increase the value of P_{cr} at high values of W_d for the cases of 1 and 2 nodes per interval.

In some cases the buckle length does not extend over $2N_j$ and the full height of the imperfection is not effective. The result of this would be a higher buckling force. This situation exists for most points of the case with $N_j = 10$, and an increase is observed in the results on Figure 7.

4.3.4 Evaluation of Error

The known error in the estimate of P_{cr} obtained by the computer should be within ±2.5%. If the RMS deviation from the correlation represents the square-root of the sum of the squares of the variations and errors from all sources, then the ±2.5% is a minor contributor to the overall variation. Additional error could occur due to the slow convergence of the iterative procedure at low values of magnitude of P_{cr}. The computer decision to increase the test load by 5% could be based on either a faulty indication of the lack of buckling when the convergence process is very slow, with resulting lack of precision in the computation, or on faulty programming which limits the cycles per load step.

Another source of error in the estimate of P_{cr} obtained by the computer can result from the numerical approximation and the small number of nodes in the short buckle length at high values of P_{cr}.

5. DISCUSSION OF RESULTS

From Figure 2 it can be seen that for the perfect system there is no apparent bifurcation point at which the trivial state and a buckled state have the same load. As the buckle height W_o approaches zero asymptotically, the equilibrium axial load approaches infinity.

For the system with a point imperfection, the presence of a bifurcation point is indicated. This occurs where the solutions for the system with a point imperfection and for the perfect system coincide, as they do when $kS = 4.4934$, $F_i = 0$, and $-W_i = -W_o$ for W_o as shown in Figure 2.

The results of this investigation of flat strips held by a transverse pressure can be compared to the results from the investigations of the behavior of a ring in a rigid cavity [3 - 7].

The results for the two systems have the following similarities:

a) Imperfections are required in both systems in order to initiate buckles with the critical buckling load approaching infinity as the imperfection approaches zero.

b) With point imperfections in both systems, the characteristic value of $kS = 4.4934$ radians = 257 deg of arc.

c) With smooth imperfections in both systems the results indicate that, before the critical point of maximum axial force is reached, the strip (or ring) lifts from the peak of the imperfection but then requires additional force to attain additional deflection until it reaches the peak force, after which the force decreases for increasing deflection.

The results obtained from the two systems show some significant differences which appear in the results, and also in the interpretation of results, shown in Figure 6 of Bucciarelli and Pian [7]:

a) For a point imperfection, the results for a ring show a first power inverse relation between buckling load and imperfection height. For the flat strip, this is a second power inverse relation. This difference can be attributed to the fact that for the ring the effective pressure q of the strip is replaced by P/R.

b) Bucciarelli and Pian [7] predict that for their assumed smooth imperfections and initial stress-free deformed condition of the ring, lifting starts with the first application of axial force. Here, however, it was found that a value of axial force almost as great as the critical buckling force is required to initiate lifting, as shown in Figure 5. This behavior of the ring can be attributed to the lack of a pressure q and to the initial stress-free deformed condition which eliminates the two initial downward components of the initial forces indicated here in eq. (4).

c) Bucciarelli and Pian [7] conclude that the smooth imperfections effect a greater reduction in axial buckling force than do sharp imperfections throughout the range of magnitude of imperfections as shown by their Figure 6. This is contrary to what was found for flat strips, as shown here in Figure 6.

This difference between predictions can possibly be explained by the fact that Bucciarelli and Pian [7] compare the behavior of a ring which is initially stress-free over a smooth imperfection to the behavior of a ring which has initial stress over a point imperfection.

The computer approach to the study of the effect of random imperfections allows for a wide variation in the types of imperfections. In this case the imperfections were uniformly spaced at regular intervals along the base with linear interpolation for intermediate nodes. The imperfections could also be non-uniformly spaced at random intervals of either uniform or Gaussian distribution and could also have curve fitting between specified imperfection points. The imperfections could be applied to the strip as well as to the base.

The range of magnitude of imperfections which can be studied is limited by practical considerations. At high values of the magnitude of the imperfections, slow growth of the buckle and excessive computer time limit the range. At low values of the magnitude of imperfections, the range is limited by high values of buckling load which reached the point of numerical instability of the equations.

The systematic variation in the results shown in Tables 1 and 2 from the effect of varying the number of nodes per imperfection deserves further study. Rather than varying the number of nodal points per imperfection, and thereby varying the number of imperfections in the base, one might use the same total number of imperfections in the base and the same number of nodal points per imperfection by varying the length of the strip. This is only feasible in the loading range where the buckle length will always include a large number of nodal points (i.e., greater than 10) so that errors due to the finite difference approximation can be minimized. The resulting system would then have a very small nodal spacing and very slow convergence.

6. CONCLUSIONS

6.1 Conclusions from Mathematical Analysis

From the results of the previous work it can be concluded that:

a) It is possible to obtain mathematical solutions for the perfect system and for the system with simple imperfections by using relatively simple techniques.

b) The system is completely imperfection sensitive. No buckles occur unless imperfections are present and the buckling force is a function of the magnitude of the imperfections.

c) With cosine wave imperfections in the base, a finite predictable axial force is required to initiate lifting of the strip. The axial force must be increased above the value of this initial lifting force before instability occurs at a critical point.

d) With cosine wave imperfections in the base, there is an optimum relation between parameters (magnitude of the wave, wave length, bending stiffness, and transverse pressure) which yields the lowest value of buckling force.

e) Contrary to the behavior predicted by Bucciarelli and Pian [7] for a ring in a rigid cavity, the effect of point imperfections in reducing the axial buckling force is greater than the effect of smooth (cosine wave) imperfections. The basis for the opposite conclusion by Bucciarelli and Pian is subject to question.

6.2 Conclusions from Analysis by Numerical Methods

The following conclusions can be drawn from the results of the analysis by numerical methods:

a) There is a simple modification which extends the Gauss-Seidel method for solutions to linear structural problems so that solutions to this non-linear problem may be obtained. It is possible that this method may be extended to problems of a more practical nature in two dimensions.

b) There is shown to exist a relation between the method for obtaining static solutions using an iterative technique and the method for obtaining dynamic solutions using a simple predictor technique. This relation allows instability to be defined on the basis of dynamic behavior.

c) The numerical method is useful in evaluating the effect of random imperfections on the buckling of an imperfection-sensitive system.

d) Within the range of random imperfections studied, the effect of random imperfections can be predicted with reasonable accuracy by relations developed from the mathematical analysis of either point imperfections or cosine wave imperfections. The RMS value of the random imperfections is substituted for the height of the simple cosine wave imperfections. The wave length of the buckle over a set of random imperfections assumes that length which yields the minimum buckling force for the assumed height of a cosine wave imperfection as above. There are systematic deviations from the predicted behavior.

6.3 Overall Conclusions

a) The problem of buckling of a strip on a rigid base, a problem of simple geometry but complex elastic stability characteristics, has been solved by mathematical analysis, and by numerical methods. The results of the two methods are in agreement.

b) The behavior of the strip has been shown to be similar to that of a ring in a rigid cavity. Mathematical solutions are less complex for the strip than for the ring.

c) The sensitivity of the strip geometry to imperfections, its unique instability characteristics, the relatively simple geometry, and the ease of obtaining numerical solutions suggest that this might provide a reasonable basis for further study of the effect of random imperfections on the buckling behavior of imperfection sensitive systems.

d) The basic aspects of this problem can have wide application in practical problems ranging from design of highway slabs and pipelines to the behavior of linings and claddings of pressure vessels and claddings of fuel elements. The numerical method of obtaining solutions appears to offer the greatest flexibility for treatment of different geometries and service conditions.

e) The possibility of inelastic behavior of the strip may be encountered in many practical problems and any solution must be examined in that light. If the system remains elastic up to the snap-through condition, this elastic solution may provide all that is required for practical engineering purposes.

APPENDIX
RELATION OF ITERATIVE CYCLES TO INCREMENTS OF TIME

Using Gauss's methods of iteration [13], the estimated value of w_i at the $(j+1)^{th}$ iteration using a convergence factor CONF and simple central differences is given by

$$w_{i,j+1} = \frac{CONF \cdot d^4}{6D - 2d^2P}\left(q - r - \frac{D}{d^4}\Delta^4 w_j - \frac{P}{d^2}\Delta^2 w_j\right) + CONF \cdot w_{i,j} + (1 - CONF) \cdot w_{i,j-1} \cdot \qquad (25)$$

Eq. (25) can be related to the finite difference equation for dynamic equilibrium at point i and time t by including the effect of viscous damping. Using simple central differences, the dynamic equation becomes

$$w_{i,t+\Delta t} = \frac{\Delta t^2}{\rho A + \frac{C_d \Delta t}{2}}\left(q - r - \frac{D\Delta^4}{d^4} w_t - \frac{P\Delta^2}{d^2} w_t\right) + 2w_{i,t}\frac{\rho A}{\rho A + \frac{C_d \Delta t}{2}} - \left(\frac{2\rho A - C_d \Delta t}{2\rho A + C_d \Delta t}\right) \cdot w_{i,t-\Delta t} \quad , \qquad (26)$$

where A is the cross-sectional area of the strip.

By equating the coefficients of the second term on the right hand side of each of eqs. (25) and (26) one obtains

$$CONF = \frac{4\rho A}{2\rho A + C_d \Delta t} \quad \text{or} \quad \frac{C_d \Delta t}{2\rho A} = \frac{2}{CONF} - 1 \, . \qquad (27)$$

Since positive damping in the dynamic system requires $C_d \Delta t / 2\rho A > 0$, then eq. (27) shows that in the iterative system it is required that CONF < 2. When CONF < 1.0, then $C_d \Delta t / 2\rho A > 1.0$, which is indicative of a highly damped system. For accelerated convergence in structural problems, the value of CONF is usually taken in the range $1.0 < CONF < 1.6$ according to White [14]. This results in a range for $C_d \Delta t / 2\rho A$ of $1.0 > C_d \Delta t / 2\rho A > 0.25$.

Equating the coefficients of the third term on the right hand side of each of eqs. (25) and (26) yields

$$CONF - 1 = \frac{2\rho A - C_d \Delta t}{2\rho A + C_d \Delta t} \, . \qquad (28)$$

Eqs. (27) and (28) are mutually satisfied only when CONF = 4/3 and $C_d \Delta t/2\rho A = 0.5$. These values are also characteristic of a highly damped system.

Using the value of CONF = 4/3 and $C_d \Delta t/2\rho A = 0.5$ and equating the coefficients of the first terms of each of eqs. (25) and (26), one can calculate an equivalent Δt_j for the change in the deflection from the j^{th} estimate to the $(j+1)^{th}$ estimate of w_i.

$$\Delta t = \left(\frac{2\rho A\, d^4}{6D - 2d^2 P} \right)^{1/2} . \qquad (29)$$

It can be seen from eq. (29) that the equivalent Δt for the iterative cycle would increase to infinity if $6D = 2d^2P$. This condition also reduces the denominator of eq. (25) to zero and results in numerical instability for the iterative method of solution.

LIST OF REFERENCES

[1] Anderson, W.F., "Structural Evaluation of Proposed ASCR Moderator Cans," NAA-SR-TDR-6082, Atomics International, A Division of North American Rockwell Corp., Canoga Park, California, January 31, 1961 (available from author).

[2] Calladine, C.R., "On the Creep of a Wrinkle," Colloquium on Creep in Structures, Springer Verlag, Berlin, 1962, pp. 245-271.

[3] Hsu Lo, Bogdanoff, J.L., Goldberg, J.E., and Crawford, R.F., "A Buckling Problem of a Circular Ring," Fourth U.S. Congress of Applied Mechanics, Berkeley, California, 1962. Edited by R.M. Rosenberg, published by ASME, United Engineering Center, New York, Vol. I, pp. 291-696.

[4] Hsu, P.T., Elkon, J., and Pian, T.H.H., "Note on the Instability of Circular Rings Confined to a Rigid Boundary," Trans. ASME, Journal of Applied Mechanics, Brief Notes, Vol. 31, Series E, No. 3, 9/64, p. 559.

[5] Elkon, Y., "Studies on the Instability of Circular Rings," Aeroelastic and Structures Research Laboratory, Massachusetts Institute of Technology, ASRL Technical Report 119-1, AFOSR 64-1843, June 1964.

[6] Chan, H.C., and McMinn, S.J., "The Stability of a Uniformly Compressed Ring Surrounded by a Rigid Circular Surface," International Journal of Mechanical Science, Vol. 8, 1966, pp. 433-442.

[7] Bucciarelli, L.L., Jr., and Pian, T.H.H., "Effect of Initial Imperfections on the Instability of a Ring Confined in an Imperfect Rigid Boundary," Trans. ASME, Journal of Applied Mechanics, Vol. 34, Series E, No. 4, December 1967, pp. 979-984.

[8] Zagustin, E.E., and Herrmann, G., "Stability of an Elastic Ring in a Rigid Cavity," Trans. ASME, Journal of Applied Mechanics, Vol. 34, Series E, No. 2, June 1967, pp. 263-270.

[9] Chicurel, R., "Shrink Buckling of Circular Rings," Trans. ASME, Journal of Applied Mechanics, Brief Notes, Vol. 35, Series E, No. 3, September 1968, p. 608.

[10] Anderson, W.F., "Buckling of a Strip on a Rigid Half-Space with a Transverse Pressure," Ph.D. dissertation, Department of Civil Engineering, University of Southern California, Los Angeles, 1971.

[11] Weitsman, Y., "On Foundations That React in Compression Only," Trans. ASME, Journal of Applied Mechanics, Vol. 37, Series E, No. 4, December 1970, pp. 1019-1030.

[12] Timoshenko, S.P., and Gere, J.M., Theory of Elastic Stability, 2nd edition, McGraw-Hill Book Co., New York, 1961.

[13] Varga, R.S., Matrix Iterative Analysis, Prentice Hall, Englewood Cliffs, New Jersey, 1962.

TABLE I

DATA AND RESULTS FROM NUMERICAL STUDIES OF BUCKLING WITH RANDOM IMPERFECTIONS OF THE BASE

Case No.	Nodes per Interval	RMS Deviation of Base (in.)	Peak Negative Imperfection (in.)	No. of Iterations at Buckle Load	No. of Iterations at Previous Load	Force at Buckle Load (lb)	Buckle Length in Nodes
1	1	0.00001	0.0000262	200	200	1548	6
2	1	0.0000158	0.0000455	250	200	1061	5
3	1	0.0000251	0.0000792	250	200	980	8
4	1	0.0000398	0.0001170	200	200	860	9
5	1	0.0000630	0.0001496	300	200	693	10
6	1	0.00010	0.000237	300	400	568	NG*
7	1	0.000158	0.000442	350	200	500	NG
8	1	0.000291	0.000807	400	300	399	11
9	1	0.000398	0.001283	500	250	322	13
10	1	0.000631	0.001797	800	200	285	15
11	1	0.0010	0.00278	500	200	256	NG
12	1	0.00158	0.00482	1000	1000	205	NG
13	1	0.00251	0.00641	800	400	179	16
14	2	0.000010	0.0000262	200	200	1612	5
15	2	0.0000158	0.0000401	200	200	1312	7
16	2	0.0000251	0.0000721	350	200	1073	NG
17	2	0.0000398	0.0001033	300	200	797	NG
18	2	0.0000631	0.0001989	250	200	662	NG
19	2	0.00010	0.000286	300	300	564	12
20	2	0.000158	0.000354	400	250	453	11
21	2	0.000251	0.000738	450	300	327	NG
22	2	0.000398	0.000944	500	300	338	NG
23	2	0.000631	0.001483	650	750	284	NG
24	2	0.0010	0.00196	250	250	260	15
25	2	0.00158	0.00376	850	1000	189	18
26	5	0.000010	0.0000262	200	200	2257	5
27	5	0.0000158	0.0000387	200	200	2144	5
28	5	0.0000251	0.0000612	200	200	1612	7
29	5	0.0000398	0.0000808	200	200	1194	8
30	5	0.0000631	0.0001595	200	200	971	8
31	5	0.00010	0.000201	250	200	730	NG
32	5	0.000158	0.000454	500	200	533	NG
33	5	0.000251	0.000651	550	200	469	NG
34	5	0.000398	0.000740	950	200	329	14
35	5	0.000631	0.001349	800	250	296	16
36	5	0.0010	0.00260	1000	1000	250	16
37	5	0.00158	0.00351	1000	1000	211	NG
38	10	0.0000158	0.0000312	50	100	2906	NG
39	10	0.0000251	0.0000492	100	100	2150	6
40	10	0.0000398	0.0001044	100	100	1638	6
41	10	0.0000631	0.0001537	100	100	1412	8
42	10	0.00010	0.000191	100	100	1123	NG
43	10	0.000158	0.000262	350	100	846	NG
44	10	0.000251	0.000510	500	100	563	NG
45	10	0.000398	0.001006	650	100	460	NG
46	10	0.000631	0.000920	800	100	372	NG
47	10	0.0010	0.00137	1000+	100	246	14
48	10	0.00158	0.00319	2550	200	205	16
49	10	0.00251	0.00721	1000+	100	173	NG

*NG = No graph from computer.

TABLE II

DATA AND RESULTS OF STATISTICAL CORRELATION BETWEEN AXIAL BUCKLING FORCE AND MAGNITUDE OF RANDOM IMPERFECTIONS

First Order Fit						Second Order Fit [$\log_{10}$(lb)]			
No. of Nodes per Interval	No. of Solutions	Intercept [$\log_{10}$(lb)]	Coefficients [$\log_{10}$(lb)]	RMS Deviation [$\log_{10}$(lb)]	Deviation of Estimate (%)	Intercept	First Coefficient	Second Coefficient	RMS Deviation
1	13	1.225	-0.385	0.0251	6	1.256	-0.367	0.00235	0.0262
2	12	1.087	-0.419	0.041	10	1.723	-0.818	0.0432	0.0374
5	12	0.866	-0.503	0.0363	8.7	1.436	-0.201	0.0387	0.0335
10	12	0.728	-0.571	0.0317	7.5	0.609	-0.637	-0.00894	0.0316
1,2,5,10	49	1.033	-0.453	0.105	27.5	1.060	-0.439	0.00190	0.106

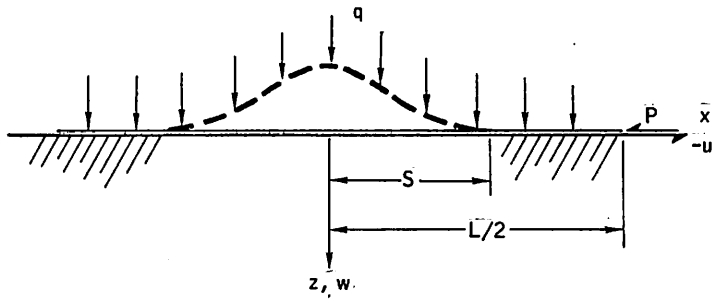

a.

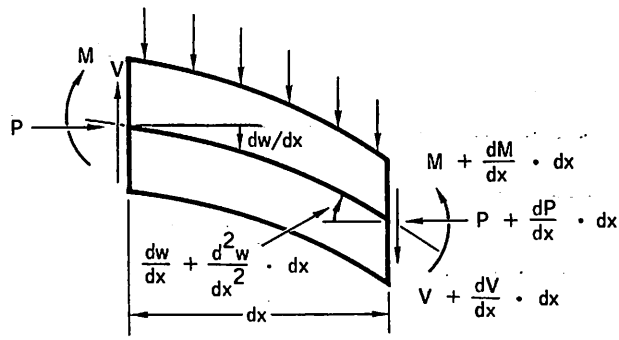

b.

LMEC-93001

1. Forces on a Buckle in a Perfect System
   a. Symmetrical Buckle
   b. Element of the Buckle not in Contact with the Base

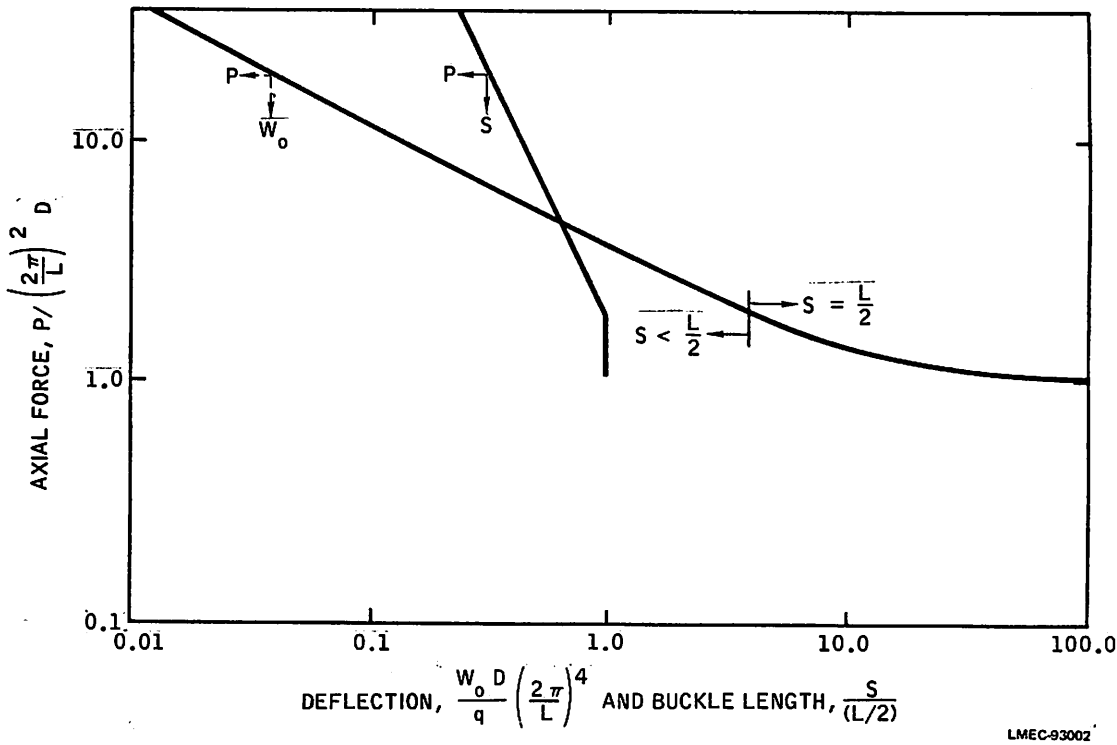

2. Axial Force — Deflection Relations and Axial Force — Buckle Length Relations for a Buckle in a Perfect System

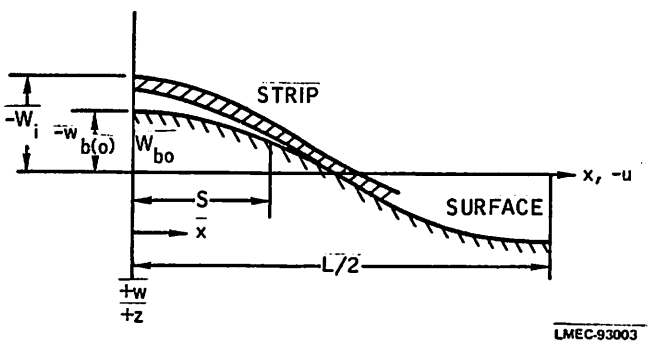

3. A Symmetrical Buckle at a Cosine Wave Imperfection of the Base

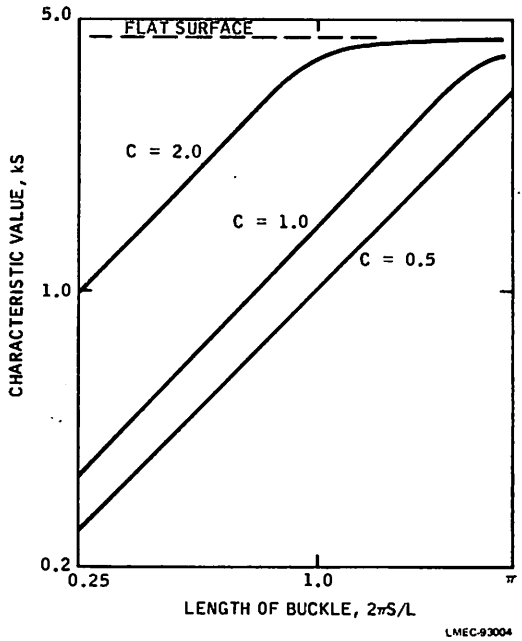

4. Characteristic Value — Buckle Length Relations with Cosine Wave Imperfections for Values of C = 0.5, 1.0, and 2.0

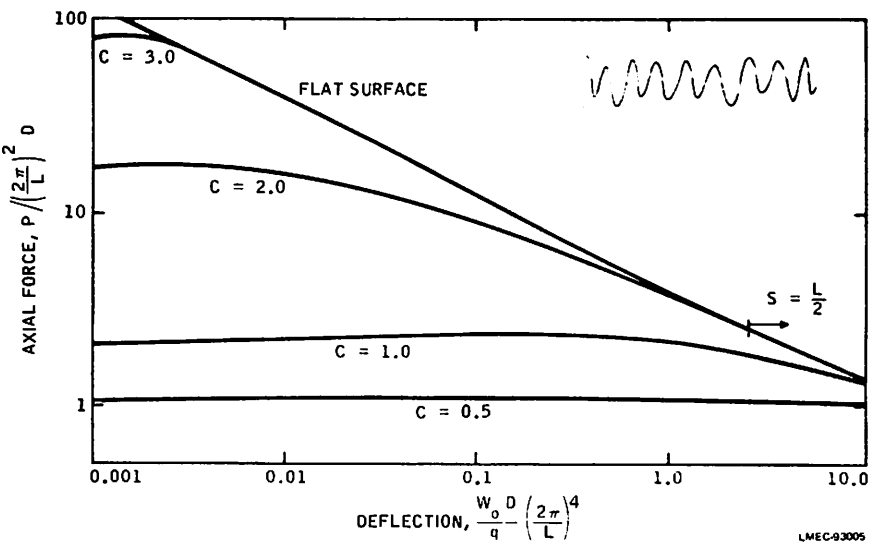

5. Axial Force — Deflection Relations with Cosine Wave Imperfections for Values of C = 0.5, 1.0, 2.0, and 3.0

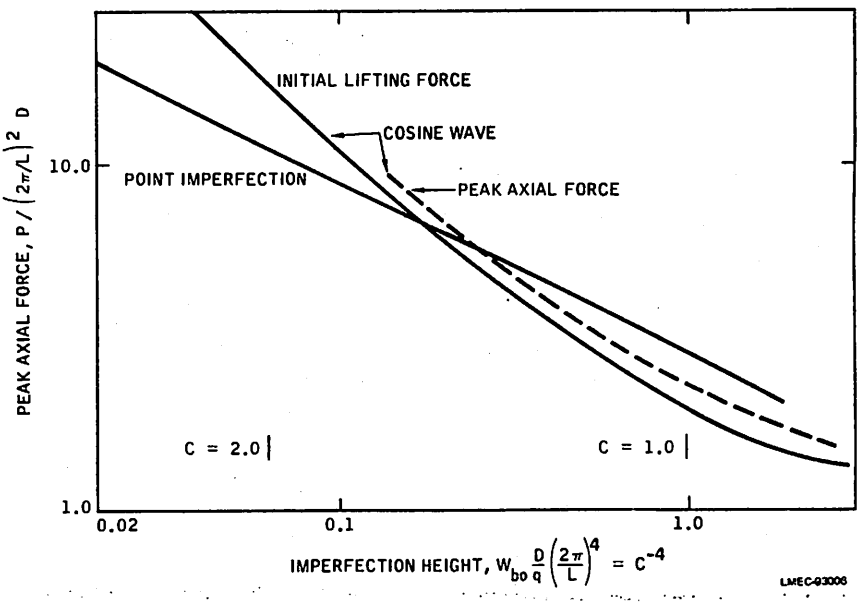

6. Peak Axial Force – Imperfection Height Relations for Cosine Wave Imperfections and Point Imperfections

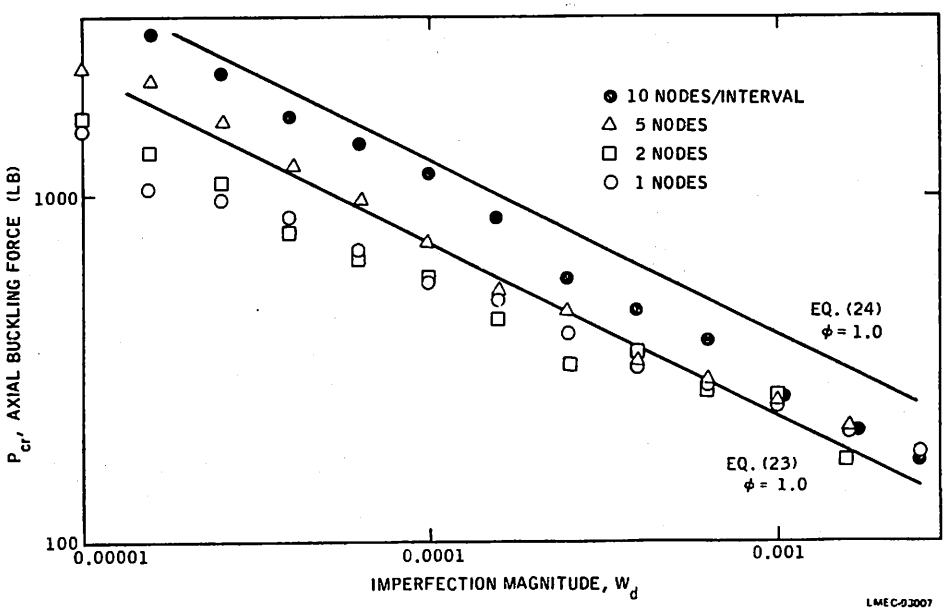

7. Axial Buckling Force – Imperfection Magnitude Relation with Random Imperfection Spacing of 1, 2, 5, and 10 Nodes

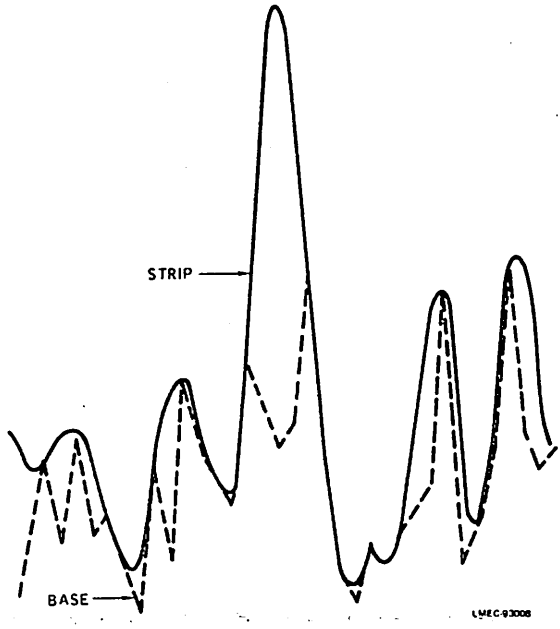

8. Configuration of a Buckle with Random Imperfection Spacing of 1 Node and W_d = 0.0000158 in.

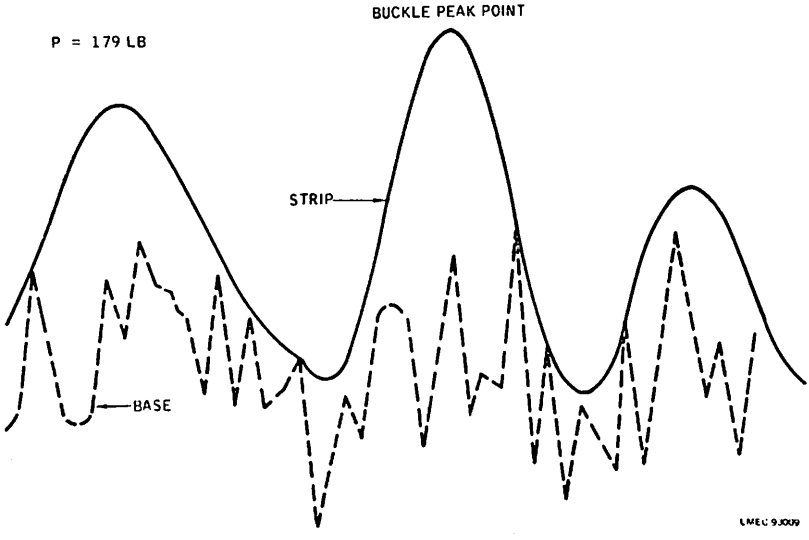

9. Configuration of a Buckle with Random Imperfection Spacing of 1 Node and W_d = 0.00251 in.

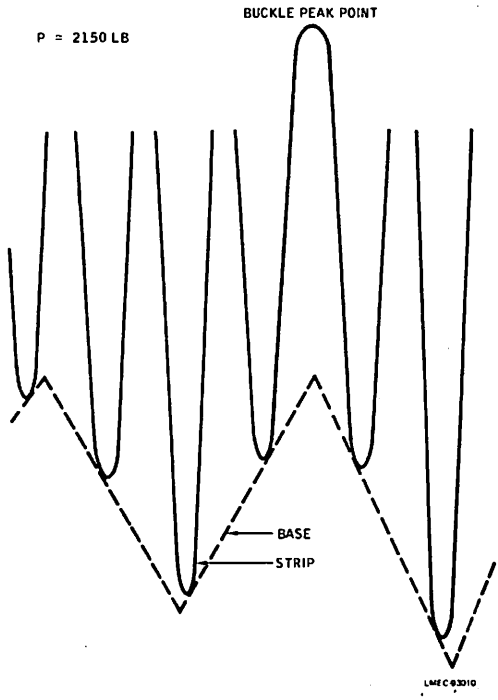

10. Configuration of a Buckle with Random Imperfection Spacing of 10 Nodes and W_d = 0.0000251 in.

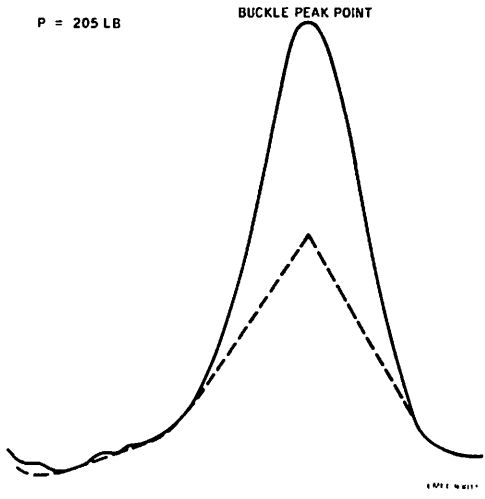

11. Configuration of a Buckle with Random Imperfection Spacing of 10 Nodes and W_d = 0.00251 in.